United States
Department of
Agriculture

Forest Service

Intermountain
Research Station

Research Paper
INT-424

July 1990

Relationship of Fuel Size and Spacing to Combustion Characteristics of Laboratory Fuel Cribs

Hal E. Anderson

THE AUTHOR

HAL E. ANDERSON has been team leader of the basic research section of the Fire Behavior: Fundamentals and Systems Development research work unit since 1979. He joined the staff at Intermountain Station's Intermountain Fire Sciences Laboratory (formerly Northern Forest Fire Laboratory) in 1961 and served as project leader of the the fire physics project from 1962 to 1966 and of the fuel science project from 1966 to 1979. He previously worked with General Electric Company from 1952 to 1961 on thermal and nuclear instrumentation. He received his B.S. degree in physics from Central Washington University in 1952. (The author retired from the Forest Service in April 1990.)

RESEARCH SUMMARY

Flaming combustion in cribs of large woody fuels, thickness 5 cm or greater, is not sustained when fuel spacing ratio, fuel edge-to-edge separation distance to fuel thickness, is greater than 3:1. The burning rate per unit of exposed fuel surface area was found to reach a maximum near a porosity of 0.21, where porosity is defined as the square root of the ratio of vertical venting area to the exposed large fuel surface area. The flame length associated with the large-fuel burning rate was found to drop rapidly when the porosity exceeds 0.3 and the large-fuel spacing ratio increases beyond 2.23:1. This supports the critical spacing assigned in the large fuel subroutine burnout of Albini's (1976b) fire modeling program.

Intermountain Research Station
324 25th Street
Ogden, UT 84401

Relationship of Fuel Size and Spacing to Combustion Characteristics of Laboratory Fuel Cribs

Hal E. Anderson

INTRODUCTION

Study of fire behavior in wildland fuels has concentrated on the dependence of the rate of spread on fuel properties, fuel moisture contents, slope, and wind (Rothermel 1972). As the knowledge base developed and use of mathematical models became more common, users expressed interest in other aspects of fire behavior. These interests included areal fire growth and size, flame length and tree crown scorch, energy release rates, and spotting distances, including fire duration and burnout properties (Albini 1976a, 1976b). A model of the mass loss history of fuels was developed by Albini that provides an estimate of the duration of flaming combustion and the fire intensity of wildland fires. The model is limited to fuel consumption during the flaming phase of the burning process. The model included an estimate of the planform fuel separation distance (2.33:1) at which a specific fuel size can no longer sustain flaming combustion in adjacent fuels.

Since several assumptions used in Albini's model have not been tested, a study was undertaken to determine the accuracy of the assumption of fuel spacing and provide additional insights into the burning rates during flaming. This paper presents results showing the dependence of the burning rate and flame length on the physical properties of square cribs of large-sized woody fuels. Fuels included square sticks, either 5.08 cm (2.0 in), 10.16 cm (4.0 in), or 15.24 cm (6.0 in) in thickness and 122 cm (4.0 ft) in length. The spacing of fuels varied from 0.5 to 3.0 times the thickness of the large fuel. Smaller fuels were used to ignite the crib and provided a measure of how the burning rate tracked combustion of each size class. Results confirm that the burning rate was affected by porosity and spacing. The variation in the burnout of fuel sizes between the burnout model and observation shows how the flaming phase changes with fuel size and spacing. The influence of moisture content was considered by burning a few cribs at about 12 percent and 20 percent moisture content. Flame length showed a sharp drop as spacing was increased and porosity became more open.

PRIOR RESEARCH

The burning of wood cribs for both spreading fires and nonspreading or area fires has been investigated for years to develop an understanding of fire behavior. Harmathy (1972a, 1972b) presented an extensive review of previous work on crib fires within enclosures and in unconfined atmospheres. That work, plus the research of others, provided a basis for evaluating certain aspects of the burnout model developed by Albini (1976b), such as investigating the effect of spacing on the flaming burnout (Block 1971; Gross 1962; Heskestad 1973; Smith and Thomas 1970; Thomas 1974). These authors pointed out that the burning rates of wood crib area fires fell into two regimes: (1) when the fuels are closely packed, the burning rate is ventilation controlled, and (2) when the fuels are quite loosely packed, the burning rate is controlled by the exposed fuel surface area. The general form has been presented by several researchers (Block 1971; Delichatsios 1976; Gross 1962; Harmathy 1972a, 1976; Heskestad 1973), but has been expressed differently because of scaling factors or because dimensionless analysis functions were used to group the variables. Smith and Thomas (1970) expressed similar observations noting a decrease in the burning rate with large spacing. This suggested that burnout of large fuels could be expressed in terms of, or a function of, the porosity. Comments following Block's paper (1971) at the 13th symposium on combustion brought out this concept in response to A. M. Kanury. Block (1971) expressed the thought that, at extremely open conditions, the burning rate would start to decrease and a series of negative sloped lines for each size would describe the dependence on porosity. Heskestad (1973) noted in his paper that the ventilation controlled curve rising toward the "constant" burning rate portion is a section of a parabola. This suggests that Block's thought about decreased burning rates in open fuel beds could be represented by a parabolic response function that covers the rising burn rate at small ventilation or porosity values and the decreasing burn rate at large ventilation or porosity values. Research on fire spread in wildland fuels for horizontal or vertical rates of spread has indicated that mass loss rates reach a maximum at a critical bulk density or packing ratio and then decline with further changes in the bulk density (Frandsen and Schuette 1978; Rothermel 1972; Wilson 1982).

Review of the above research indicated that, in both the ventilation-controlled and the surface-area-controlled regions, the mass loss rate per unit area of exposed fuel surface is basically a function of the ratio of ventilation area to exposed fuel surface area to the one-half power.

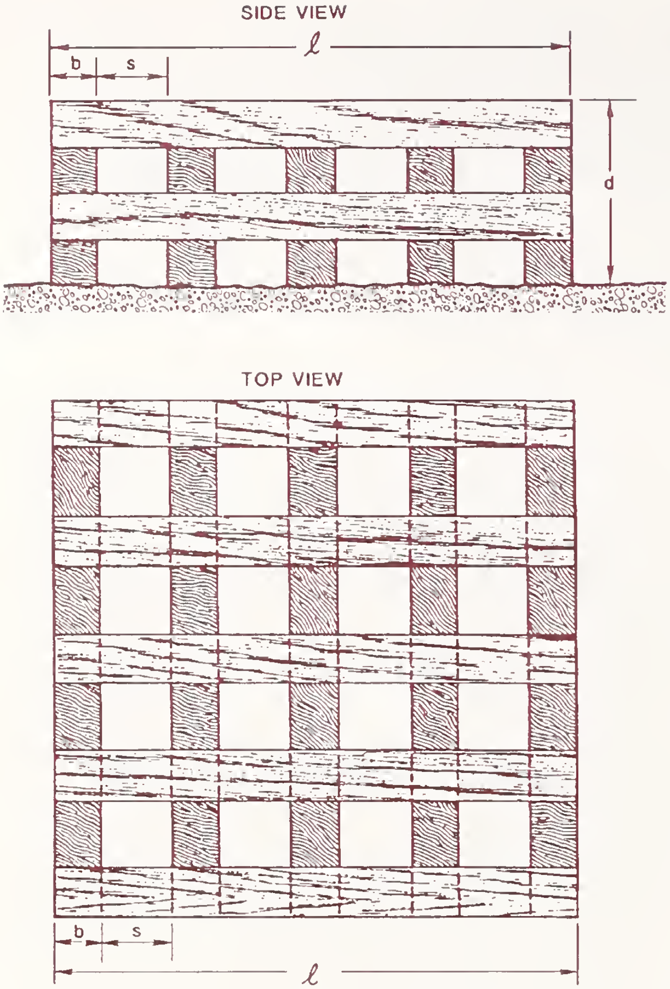

Figure 1—General configuration of large fuel in wood crib used to study the flaming burnout properties of fires. Thickness is denoted by *b*, spacing of pieces by *s*, length of pieces by ℓ, and depth of the fuel bed by *d*.

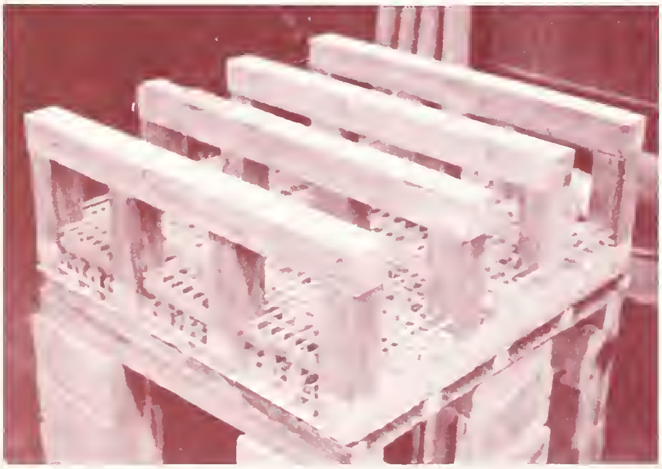

Figure 2—An oblique view of a fuel bed being constructed. Shows the arrangement of fine fuels between the large fuels and the horizontal and vertical spacing of the large fuels.

This ratio is a major term known as the porosity factor (Gross 1962; Heskestad 1973), and can be expressed mathematically as:

$$R_r/A_s = f\,(A_v/A_s) \qquad (1)$$

where R_r = mass loss rate per unit area of fuel surface, g/s
A_s = area of exposed fuel surface, cm²
A_v = cross-section area of vertical vents in the crib, that is, the planform area not occupied by fuel, cm².

This relation provides a basis for evaluating how burning rate changes as the fuel bed becomes more and more open.

The exposed surface area of the large fuels was determined from the total surface area by subtracting from it the surface area of the perimeter outward-facing sides of the pieces, the surface area of the top and bottom layers' outward-facing sides, and the surface areas that are covered at each intersection of the pieces. These outward-facing and shielded surface areas were subtracted from the total surface area because they do not interact with the fire in the fuel arrangement. The general geometry is shown in figure 1 for a fuel bed where the spacing is only horizontal. When vertical spacing equal to the horizontal spacing is desired, large fuel pieces equal to the spacing distance in length are used to separate each layer of large fuels (fig. 2). For horizontal spacing the equation for the exposed surface area is:

$$A_{sh} = 2N(n-1)b\,\ell + 2(N-1)n(b\,\ell^2 - nb^2) \qquad (2)$$

where b = fuel stick thickness, cm
ℓ = fuel stick length, cm, also fuel bed width
n = number of sticks per layer
N = number of layers.

When vertical spacing is added, the equation for the additional exposed surface area is:

$$A_{sv} = 4bsn(n-1)\,(N-1) \qquad (3)$$

where s = the spacing distance, cm, and the length of support pieces of the large fuel.

The vertical venting area was determined from the spacing and the number of pieces:

$$A_v = (n-1)^2\, s^2 \text{ cm}^2 \qquad (4)$$

This paper reports on the relationship of the burning rate to changes in the fuel stick size, spacing, and resulting fuel bed porosity.

EXPERIMENTAL PROCEDURES

The experiments were conducted using squared sticks positioned at specific distances from one another in square cribs that had a maximum base of 122 cm (4.0 ft) on a side. Fuel sizes included starter fuels used to bring the large fuels into combustion in a manner similar to the burning process observed in the field. These fuels included 0.07-cm (0.027-in)-thick excelsior of aspen wood (*Populus tremuloides* Michx.), 0.635-cm (0.25-in) and 2.54-cm (1.0-in) sticks of ponderosa pine (*Pinus ponderosa* Laws.), or sugar pine (*Pinus lambertiana* Dougl.).

Larger fuels were one of the following sizes: 5.08-cm (2.0-in), 10.16-cm (4.0-in), and 15.24-cm (6.0-in) square sticks of ponderosa pine, Douglas-fir (*Pseudotsuga menziesii* [Mirb.] Franco), or lodgepole pine (*Pinus contorta* Dougl.); or a mixture of Engelmann spruce (*Picea engelmannii* Parry) and subalpine fir (*Abies lasiocarpa* [Hook.] Nutt.). The fuels in a majority of the experimental burns were conditioned to 6 percent moisture content (mc) oven-dry (OD). A few of the burns, however, had the large fuels conditioned at 11 to 14 percent mc OD and 20 to 22 percent mc OD. An initial series of burns was carried out to determine the burnout characteristics of the 2.54-cm (1-in) fuels because their burnout would be considered a reference for the burning rate of the larger fuels. Spacing of the 2.54-cm (1-in) fuels was varied vertically and horizontally to establish how the small fuels would be distributed. As a result the 0.63-cm (1/4-in) sticks were spaced at a spacing ratio, spacing distance to fuel thickness, of 8:1 and the 1-inch sticks at a ratio of 5:1 for all the burns. For the larger fuels the spacing was varied from a low ratio of 0.5:1 to a high ratio of 3:1. Physical properties of the fuel beds are presented in table 1, and each burn is identified by a sequence of properties: species; thickness (b); spacing ratio (sr); number of pieces per layer (n); number of layers (N); horizontal, H, or horizontal and vertical, HV, spacing; and percent mc.

Table 1—Identification of each test fire by species, thickness (b), spacing ratio (sr), number of pieces per layer (n), number of layers (N), piece orientation (H or HV), moisture content (mc), and physical properties of each crib

Item	Species	Thickness b	Spacing ratio sr	No. per layers n	No. of layers N	Type of spacing	Moisture content mc	Stick length ℓ	Crib depth d	Total weight Wt	Large fuel weight Wl
		cm					Percent	- - - - - cm - - - -		- - - - - kg - - - - -	
1	DF	5.08	1.00	12	4	H	6.0	116.0	20.3	78.30	70.30
2	PP	5.08	1.00	12	4	H	6.0	116.0	20.3	61.40	53.20
3	LP	5.08	1.50	10	4	H	6.0	119.0	20.3	51.20	43.00
4	SF	5.08	2.23	8	4	H	6.0	121.0	20.3	45.70	36.80
5	DF	5.08	2.23	8	4	H	6.0	121.0	20.3	57.30	46.20
6	LP	5.08	2.23	8	4	H	6.0	121.0	20.3	44.10	35.40
7	PP	5.08	2.23	8	4	H	6.0	121.0	20.3	46.30	37.20
8	PP	5.08	3.00	6	4	H	6.0	106.0	20.3	32.00	24.80
9	SF	10.16	.50	8	4	H	6.0	116.0	40.6	160.00	146.00
10	LP	10.16	1.50	5	4	H	6.0	111.0	40.6	98.80	83.30
11	PP	10.16	1.50	5	4	H	6.0	111.0	40.6	102.00	88.70
12	SF	10.16	2.00	4	4	H	6.0	101.0	40.6	72.30	58.70
13	DF	10.16	2.50	4	4	H	6.0	116.0	40.6	105.00	86.50
14	LP	10.16	2.50	4	4	H	6.0	116.0	40.6	88.00	71.10
15	PP	10.16	2.50	4	4	H	6.0	116.0	40.6	93.00	77.80
16	PP	15.24	.67	5	4	H	6.0	116.0	60.9	217.00	198.00
17	PP	15.24	1.00	4	4	H	6.0	106.0	60.9	164.00	147.00
18	PP	15.24	2.50	3	3	H	8.0	121.0	45.7	106.00	90.70
19	PP	15.24	2.50	3	4	H	8.0	121.0	60.9	161.00	138.00
20	SF	5.08	.50	16	4	H	11.5	119.0	20.3	81.90	73.40
21	LP	5.08	.50	16	4	H	22.0	119.0	20.3	95.90	85.70
22	DF	5.08	3.00	6	4	H	20.4	106.0	20.3	41.90	32.10
23	PP	5.08	2.50	7	4	H	20.0	111.0	20.3	39.50	31.30
24	DF	10.16	1.00	6	4	H	13.7	111.0	40.6	152.00	135.00
25	DF	10.16	1.00	6	4	H	22.0	111.0	40.6	152.00	135.00
26	LP	10.16	2.50	4	4	H	20.0	116.0	40.6	102.00	85.70
27	SF	15.24	2.50	3	4	H	20.0	121.0	60.9	170.00	146.00
28	PP	5.08	1.00	12	4	HV	6.0	121.0	35.5	81.10	64.80
29	PP	5.08	1.50	10	3	HV	6.0	121.0	33.0	78.30	50.30
30	PP	10.16	1.00	7	4	HV	6.0	121.0	71.1	188.00	163.00
31	PP	10.16	2.50	4	3	HV	6.0	121.0	83.8	159.00	94.60
32	PP	15.24	.75	5	3	HV	6.0	121.0	71.1	235.00	209.00
33	PP	15.24	1.50	4	3	HV	6.0	121.0	93.9	199.00	170.00
				Data Used From Gross							
34	DF	1.90	.50	7	10	H	9.2	19.0	19.0	2.11	2.11
35	DF	1.90	1.25	5	10	H	9.2	19.0	19.0	1.53	1.53
36	DF	1.90	3.50	3	10	H	9.2	19.0	19.0	.91	.91
37	DF	1.90	.50	7	7	H	9.2	19.0	13.3	1.49	1.49
38	DF	1.90	1.25	5	7	H	9.2	19.0	13.3	1.06	1.06
39	DF	1.90	3.50	3	7	H	9.2	19.0	13.3	.64	.64
40	DF	1.90	.50	7	5	H	9.2	19.0	9.5	1.05	1.05
41	DF	1.90	1.25	5	5	H	9.2	19.0	9.5	.75	.75
42	DF	1.90	.50	7	3	H	9.2	19.0	5.7	.65	.65
43	DF	1.90	1.25	5	3	H	9.2	19.0	5.7	.45	.45
44	DF	2.54	.50	7	10	H	9.2	25.4	25.4	5.97	5.97
45	DF	2.54	1.25	5	10	H	9.2	25.4	25.4	4.15	4.15
46	DF	2.54	3.50	3	10	H	9.2	25.4	25.4	2.57	2.57
47	DF	3.81	.50	7	10	H	9.2	38.1	38.1	18.60	18.60
48	DF	3.81	1.25	5	10	H	9.2	38.1	38.1	13.50	13.50
49	DF	9.15	.29	8	10	H	9.2	91.5	91.5	315.00	315.00
50	DF	9.15	.50	7	10	H	9.2	91.5	91.5	262.00	262.00

Weight loss per unit time was measured with a four-station load cell/strain gauge instrumentation setup that included heat isolation materials, a support platform, and the fuel bed. Flame height (fig. 3) was observed by three individuals making independent measurements, which were recorded on small cassette tape recorders. These observations were later coordinated and the average flame height over time included as part of the data base. In addition, two remote-controlled cameras recorded flame height at specific time intervals as set up within a microcomputer/controller. Radiant heat signatures for each fire were measured with radiometers located (1) at right angles to the flame plume, at the fuel bed height above the combustion laboratory floor; (2) at a height of 493 cm (16 ft 2 in) above the combustion laboratory floor, and 503 cm (16 ft 6 in) from the center line of the fuel bed on a line-of-sight angle of 40 degrees from the horizontal. The temperature in the base of the fuel bed was estimated with a chromel-alumel thermocouple placed approximately 30.48 cm (1.0 ft) into the fuel bed. The temperature of a load cell was monitored so correction could be made for thermal drift of the weight loss millivolt signal. All of the sensor electronic signals were collected and stored on a compact data collection unit, and after each burn the data were stored on tape and later included in a data base.

The individual observers were instructed to note each significant change that occurred during the burnout of the fuel bed. The time of each event was recorded on the tape recorders. The three observers were utilized through the flaming phase, which generally did not exceed 60 minutes. During the charring or glowing phase, one individual made observations until the fuel had totally burned out, leaving less than 5 percent of the area covered with embers. Among the significant observations were: the collapse and burnout of each of the starter fuel sizes, flame height at each observation, buildup of burning in the fuel bed, the fraction of large fuel flaming, the start of collapse, the fraction of collapse, the time when flame height above the fuel bed dropped below 30.48 cm (1.0 ft), the fraction of the fuel bed planform area in flaming or glowing, and the time when flaming and glowing ended. These observations were compared with the fractional weight-loss rate determined from the weight-loss record so that significant events in burning behavior could be evaluated in terms of weight-loss rate. The data related to the large-fuel burning rate are listed in table 2 and cover the period when the large-fuel burning dominates.

Figure 3—Burnout of experimental fuel bed. Flame lengths and the burnout of each size class of fuels were observed both visually and photographically.

Table 2—Burning rate, flame length, and other combustion characteristics determined during the burning of large fuel wood cribs

Identification of cribs	P Burn frac. sec-1	Ash hor. surf. area	Asv ver. surf. area	As-tot. tot. surf. area	Av vent area	P Porosity	Rr/As-tot. Unit area burn rate	Time of burn rate	Flame length	Frac. tot. bed remaining	Frac. large fuel remaining	Time to flame <1 ft	Tot. burn time	Residue left
Species-b-sr-n-N-/orient-mc	*sec-1*	*cm²*	*cm²*	*cm²*	*cm²*	—	*g/s-cm²*	*min*	*cm*	—	—	*min*	*min*	*gm*
DF- 5.08-1.00-12-4-H- 6.0	0.000816	72600	0	72600	3120	0.207	0.000790	11.00	274.0	0.486	0.581	29.0	128.0	–
PP- 5.08-1.00-12-4-H- 6.0	.000961	72600	0	72600	3120	.207	.000704	8.00	335.0	.414	.477	19.0	104.0	–
LP- 5.08-1.50-10-4-H- 6.0	.001110	64500	0	64500	4700	.269	.000740	8.40	335.0	.399	.475	20.0	89.0	–
SF- 5.08-2.23- 8-4-H- 6.0	.000703	54500	0	54500	6290	.339	.000475	9.00	243.0	.236	.293	15.0	112.0	–
DF- 5.08-2.23- 8-4-H- 6.0	.000682	54500	0	54500	6290	.339	.000578	9.00	304.0	.466	.578	17.0	94.0	–
LP- 5.08-2.23- 8-4-H- 6.0	.000840	54500	0	54500	6290	.339	.000547	9.60	182.0	.303	.376	23.0	73.0	–
PP- 5.08-2.23- 8-4-H- 6.0	.000622	54500	0	54500	6290	.339	.000425	8.33	243.0	.305	.378	14.1	95.0	–
PP- 5.08-3.00- 6-4-H- 6.0	.000473	35600	0	35600	5800	.403	.000330	9.00	97.5	.277	.359	11.5	89.0	322.0
SF-10.16-0.50- 8-4-H- 6.0	.000365	83800	0	83800	1260	.122	.000639	8.94	335.0	.814	.871	56.0	211.0	1010.0
LP-10.16-1.50- 5-4-H- 6.0	.000632	54900	0	54900	3710	.260	.000960	8.25	304.0	.582	.690	34.0	121.0	–
PP-10.16-1.50- 5-4-H- 6.0	.000516	54900	0	54900	3710	.260	.000835	9.63	274.0	.498	.572	24.0	132.0	712.0
SF-10.16-2.00- 4-4-H- 6.0	.000410	39600	0	39600	3710	.306	.000608	9.47	91.4	.591	.717	15.2	175.0	590.0
DF-10.16-2.50- 4-4-H- 6.0	.000384	47000	0	47000	5800	.351	.000706	7.42	182.0	.671	.794	18.0	286.0	2950.0
LP-10.16-2.50- 4-4-H- 6.0	.000371	47000	0	47000	5800	.351	.000561	8.70	121.0	.574	.710	15.5	151.0	681.0
PP-10.16-2.50- 4-4-H- 6.0	.000298	47000	0	47000	5800	.351	.000494	8.00	118.0	.821	1.000	10.0	238.0	–
PP-15.24-0.67- 5-4-H- 6.0	.000365	75500	0	75500	1660	.148	.000960	9.00	365.0	.786	.860	55.6	225.0	–
PP-15.24-1.00- 4-4-H- 6.0	.000371	55600	0	55600	2090	.193	.000987	9.00	304.0	.740	.819	30.0	242.0	1180.0
PP-15.24-2.50- 3-3-H- 8.0	.000204	36200	0	36200	5800	.400	.000512	8.90	30.4	.753	.884	8.9	376.0	–
PP-15.24-2.50- 3-4-H- 8.0	.000194	50600	0	50600	5800	.338	.000531	9.00	45.7	.719	.838	8.9	272.0	998.0
SF- 5.08-0.50-16-4-H-11.5	.000464	91300	0	91300	1450	.126	.000373	26.00	247.0	.392	.438	58.3	166.0	667.0
LP- 5.08-0.50-16-4-H-22.0	.000150	91300	0	91300	1450	.126	.000141	58.00	85.3	.250	.280	99.0	192.0	1530.0
DF- 5.08-3.00- 6-4-H-20.4	.000399	35600	0	35600	5800	.403	.000360	21.30	15.2	.410	.535	14.3	90.0	418.0
PP- 5.08-2.50- 7-4-H-20.0	.000525	43500	0	43500	5800	.365	.000379	18.20	30.4	.317	.399	22.2	117.0	–
DF-10.16-1.00- 6-4-H-13.7	.000394	63900	0	63900	2580	.200	.000831	11.00	304.0	.790	.888	40.7	223.0	989.0
DF-10.16-1.00- 6-4-H-22.0	.000243	63900	0	63900	2580	.200	.000516	21.30	213.0	.691	.776	36.0	218.0	8440.0
LP-10.16-2.50- 4-4-H-20.0	.000325	47000	0	47000	5990	.357	.000592	9.93	30.4	.635	.759	15.5	200.0	3000.0
SF-15.24-2.50- 3-4-H-20.0	.000162	50600	0	50600	5800	.338	.000469	8.78	27.4	.793	.925	5.0	690.0	2870.0
PP- 5.08-1.00-12-4-HV-6.0	.000959	76700	40800	117500	3120	.201	.000528	8.90	304.0	.358	.448	17.7	120.0	–
PP- 5.08-1.50-10-3-HV-6.0	.000855	47800	27800	75600	4700	.313	.000568	10.50	60.9	.178	.276	18.8	120.0	–
PP-10.16-1.00- 7-4-HV-6.0	.000483	81100	52000	133100	3710	.214	.000592	11.00	304.00	.507	.586	16.7	230.0	1430.0
PP-10.16-2.50- 4-3-HV-6.0	.000383	35500	26300	61800	6550	.429	.000586	8.27	152.00	.512	.861	10.5	119.0	1270.0
PP-15.24-0.75- 5-3-HV-6.0	.000325	58500	27800	86300	2090	.188	.000786	8.33	365.0	.739	.830	20.3	323.0	–
PP-15.24-1.50- 4-3-HV-6.0	.000370	48300	33400	81700	4700	.312	.000773	6.00	30.4	.726	.850	6.0	246.0	–
Date Used From Gross														
DF- 1.90-0.50- 7-10-H-9.2	.000900	5690	0	5690	32.4	.0755	.000333	–	–	–	–	–	–	–
DF- 1.90-1.25- 5-10-H-9.2	.002220	4510	0	4510	89.8	.1410	.000752	–	–	–	–	–	–	–
DF- 1.90-3.50- 3-10-H-9.2	.002170	2800	0	2800	176.0	.2500	.000700	–	–	–	–	–	–	–
DF- 1.90-0.50- 7- 7-H-9.2	.001130	3940	0	3940	32.4	.0907	.000427	–	–	–	–	–	–	–
DF- 1.90-1.25- 5- 7-H-9.2	.002230	3100	0	3100	89.8	.1700	.000761	–	–	–	–	–	–	–
DF- 1.90-3.50- 3- 7-H-9.2	.002100	1920	0	1920	176.0	.3030	.000697	–	–	–	–	–	–	–
DF- 1.90-0.50- 7- 5-H-9.2	.001480	2770	0	2770	32.4	.1080	.000560	–	–	–	–	–	–	–
DF- 1.90-1.25- 5- 5-H-9.2	.002250	2160	0	2160	89.8	.2030	.000781	–	–	–	–	–	–	–
DF- 1.90-0.50- 7- 3-H-9.2	.002050	1600	0	1600	32.4	.1420	.000833	–	–	–	–	–	–	–
DF- 1.90-1.25- 5- 3-H-9.2	.002150	1220	0	1220	89.8	.2700	.000795	–	–	–	–	–	–	–
DF- 2.54-0.50- 7-10-H-9.2	.000710	10100	0	10100	58.0	.0755	.000416	–	–	–	–	–	–	–
DF- 2.54-1.25- 5-10-H-9.2	.001340	8060	0	8060	160.0	.1410	.000689	–	–	–	–	–	–	–
DF- 2.54-3.50- 3-10-H-9.2	.001390	5010	0	5010	316.0	.2500	.000711	–	–	–	–	–	–	–
DF- 3.81-0.50- 7-10-H-9.2	.000760	18100	0	18100	362.0	.1410	.000565	–	–	–	–	–	–	–
DF- 3.81-1.25- 5-10-H-9.2	.000530	22900	0	22900	129.0	.0753	.000430	–	–	–	–	–	–	–
DF- 9.15-0.29- 8-10-H-9.2	.000180	141000	0	141000	333.0	.0485	.000401	–	–	–	–	–	–	–
DF- 9.15-0.50- 7-10-H-9.2	.000220	132000	0	132000	751.0	.0754	.000436	–	–	–	–	–	–	–

RESULTS

Because these fuel beds were made up of several fuel sizes, the contribution of the small fuels to the flaming and the weight loss was analyzed and the burnout of the 2.54-cm (1.0-in) fuels, 70 percent or more, gave the most consistent benchmark for the period where the burning and flaming was dominated by the large sized fuel. The fractional weight-loss rate was plotted against the time since ignition (fig. 4). The observed events were noted on the plot and assisted in the identification of the fractional weight loss rate associated with the large-fuel flaming burnout. The data presented by Gross (1962) for horizontally spaced fuels provided data points in the ventilation controlled region. These data points were merged with the data of the current study and used in equations 2, 3, and 4 to indicate how the unit exposed area burning rate changes with the porosity function. While Gross (1962) (fig. 5), Harmathy (1972a), Heskestad (1973), and Block (1971) have shown the unit surface area burning rate to increase with increasing porosity function in the ventilation-controlled region and to become steady in the surface-area-controlled region, this study shows the unit exposed area burning rate decreases when the porosity function becomes large (fig. 5). No clear separation of fuel size influence was found.

Distribution of the data points suggests that a parabolic or quadratic equation could describe the change in unit area burning rate with increasing porosity. The best fit was obtained with a quadratic equation which had the following expression:

$$R_r/A_s = -4.1273 \times 10^{-6} + 7.1923 \times 10^{-3}(P) - 1.6726 \times 10^{2}(P)^2 \qquad (5)$$

$$R^2 = 0.7717$$

with the predicted value and the 95 percent confidence limits illustrated in figure 6. Fuel beds with horizontal and vertical spacing of large fuels had burn rates similar to that for horizontally spaced fuels. Burns at high moisture contents had more variability in burning rates, and they tend to decrease with increasing moisture. The peak unit area burning rate occurs at a porosity of about 0.22, which yields a value of 0.000789 g/cm^2–s. That is different from the steady rate of 0.00062 gm/cm^2–s previously reported. Evaluation of burning rate in other fuels, such as slash beds in the field, in terms of porosity are difficult because of the several dimensions that are needed. To simplify estimation of burning rates, I considered the physical properties Wilson (1982) introduced, $\sigma\beta\delta$, where σ is the fuel particle surface area-to-volume ratio, cm^2/cm^3; β is the packing ratio defined by the ratio of fuel bed bulk density to fuel particle density; and δ is the depth of the fuel bed, cm. These variables can be readily measured or reasonably estimated. To obtain comparable results, the inverse of $\sigma\beta\delta$ must be used so as to produce a ratio of planform area to fuel surface area. The difference is in the planform area. The porosity function uses the vent planform area while the $\sigma\beta\delta$ function uses the fuel bed planform area. The expected result is less correlation when the fuel bed planform area is used. This is true for the polynominal fit to data and can be seen in the curve fit (fig. 7).

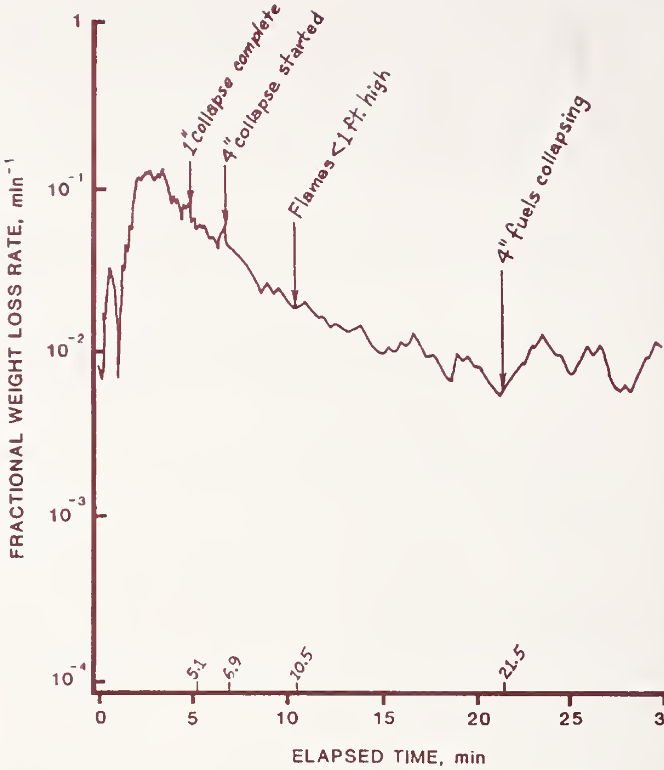

Figure 4—A plot of the fractional weight loss rate from the time of ignition to burnout. Significant events during the fire were noted by observers.

$$R_r/AS_{tot} = -4.56505 \times 10^{-5} + 2.717368 \times 10^{-3}(1/\sigma\beta\delta)^{.5} + 1.569299 \times 10^{-3}(1/\sigma\beta\delta) - 2.23657 \times 10^{-2}(1/\sigma\beta\delta)^2 \qquad (6)$$

$$R^2 = 0.6957$$

The same type of response was found in the independent observations of flame length made during each fire. The flame height associated with burning rate per unit area of exposed large-fuel surface area was found to display a sharp decrease at porosities above 0.3 (fig. 8a). Flame length values for the three large-fuel sizes, 5, 10, and 15 cm, range along a steep line between porosity values of 0.30 and 0.40. Generally, the fuel beds near this porosity did not support flaming combustion long, but did have a long smothering pyrolysis period prior to going into the glowing combustion phase of the burnout.

Similar data distribution is exhibited when flame length is plotted against the fuel bed descriptor, $1/\sigma\beta\delta$ (fig. 8b). The shifts along the axis result in part from the variation in β because of species differences in specific gravity. Species may also have other influences on volatile production and combustion, but data are insufficient to support any conclusions. Gross's (1962) data did not include measurements of flame length, thus expected flame lengths can be inferred only by use of the break point between the ventilation-controlled section and the exposed surface area section shown in figure 5. The dotted lines in figures 8a and 8b are positioned by this inference, assuming flame length nears zero when the porosity function or the fuel bed descriptor approaches zero.

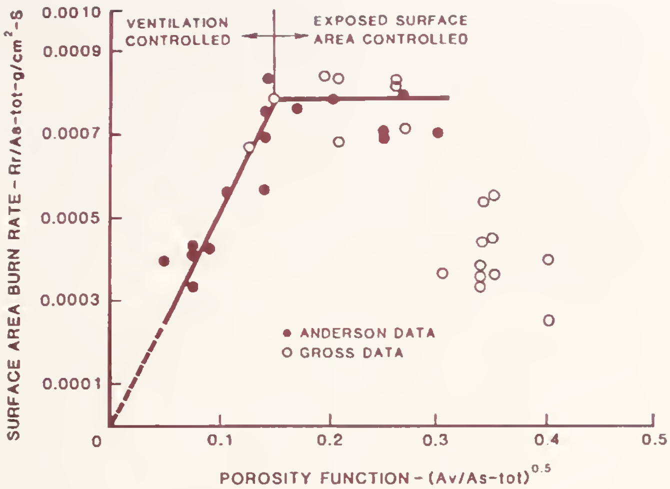

Figure 5—Relationship of surface area burning rate to porosity function. The surface area burning rate increases in the ventilation = controlled region to a maximum near 0.00078 g/cm²–s which holds nearly constant until the porosity function increases to 0.30 or greater where the burning rate decreases. Closed circles are data from Gross (1962) and open circles are data from the current study.

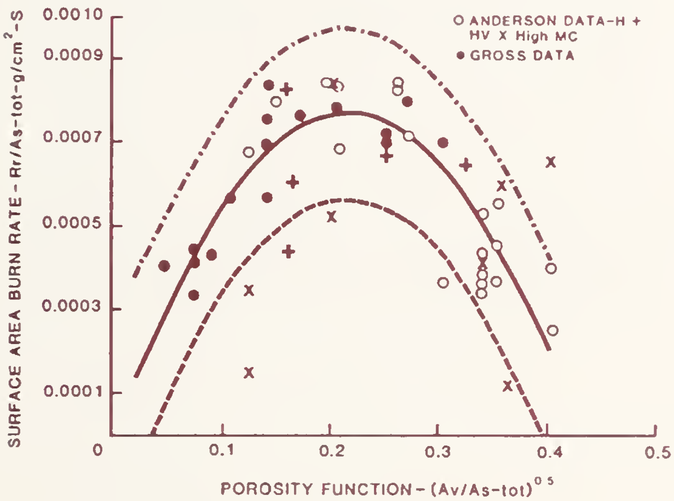

Figure 6—The response of the surface area burning rate to changing porosity. This phenomenon can be modeled by a quadratic equation—equation 4—shown by the solid line. The 95 percent confidence limits are shown by the dotted lines. The closed circles are data from Gross (1962), the open circles are data from the current study for fuels at mc less than 10 percent with horizontal spacing only, the plus symbols are for fuels with mc less than 10 percent and vertical and horizontal spacing, and the crosses are for fuels with horizontal spacing and mc greater than 10 percent.

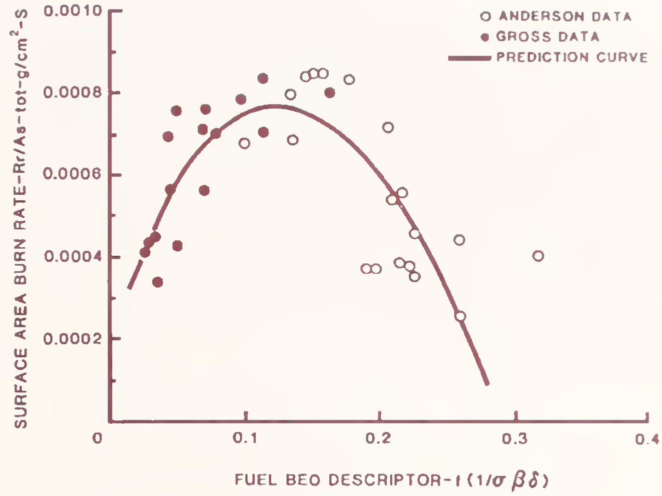

Figure 7—Relationship of surface area burning rate to fuel bed description. The surface area burning rate can be predicted by a quadratic equation—equation 5—in terms of a fuel bed descriptor, 1/σβδ , and is more suited to field application. Symbols are the same as in figure 5.

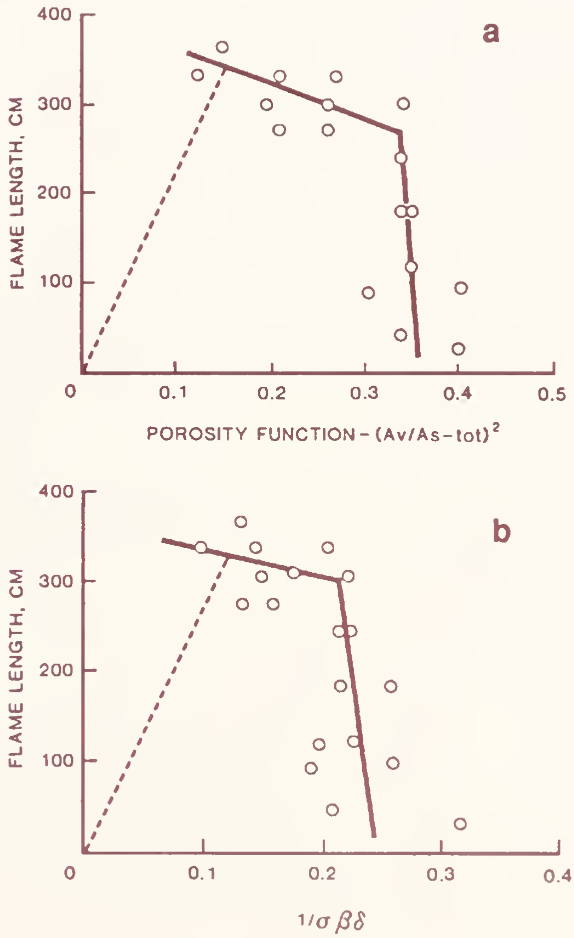

Figures 8a and 8b—Relationship of flame length to porosity and fuel bed descriptor. Flame length shows the same decrease as the burning rate as porosity or the fuel bed descriptor increases. A sharp decrease in flame length occurs at a porosity of 0.34 or a fuel bed descriptor value of 0.22. Data are from current study only.

A limited number of burns were conducted with large fuels at higher moisture contents to examine the resultant change in burning properties. Moisture contents of 11 to 14 percent and 20 to 22 percent were established for some burns, as documented in tables 1 and 2. Except for two fires at 11 to 14 percent mc, the fires were close to the curve that describes the quadratic equation for R_r/A_s as a function of the porosity (fig. 6). An estimate of the burning rate is possible with equation 4, but it is unknown whether it would apply to higher mc's. In the Pacific Northwest some prescribed burning is being done when mc's in large uncured fuels range from 63 to 113 percent (Ottmar 1987).

Some burns were conducted where the large fuels were spaced vertically and horizontally to evaluate the effect on burning rate. The results indicate that slightly higher unit area burning rates occur with spacing in both dimensions (table 2).

DISCUSSION AND SUMMARY

The critical spacing value of 2.23:1 assigned by Albini (1976b) appears to be close to the maximum spacing for large fuels for sustaining the flaming combustion phase of fuel burnout and corresponds to a porosity factor near 0.34 or a fuel bed descriptor value of 0.22. The current work indicates the 5-, 10-, and 15-cm (2-, 4-, and 6-in)-thick fuels cluster as the unit area burning rate decreases with increasing porosity or fuel bed descriptor. A porosity value of 0.34 seems to be very close to the limit of flaming combustion for large fuels, those greater than 2.54 cm (1.0 in) in thickness. Although flaming combustion may not be supported, the large fuels continue to pyrolyze and char, causing the release of numerous gaseous products until the large fuels have been consumed.

At 6 percent mc, all of the fuel beds were very nearly consumed but total consumption took up to 4 hours or more. At higher moisture contents the large fuels do not completely burn up and residues remain (table 2). Ottmar (1987) pointed out that large-fuel reduction is a function of the internal moisture content where the reduction was measured as the diameter reduction. The current work shows only the initial results for dry fuels; as fuels increase in moisture, the amount unburned will increase (table 2). Experience suggests that although moisture content influences the burnout, once pyrolysis is established large fuels burn rather completely up to 20 percent mc.

The experimental results of this study indicate that area burning rate eventually peaks and that this occurs in the vicinity of a porosity of 0.22 (fig. 6). The maximum value of 0.00078 g/cm²–s is near the value of 0.00062 g/cm²–s reported for the surface area controlled region of porosity. Earlier work in the modeling of wildland free-burning fires (Rothermel 1972) indicated that there can be optimum burning conditions where the fire reaction intensity may peak. Wilson (1982), in his reexamination of data from spreading fire, did not find well-defined peaks but rather broad indefinite peaks as reaction intensity was evaluated in terms of packing ratio. He stated that stationary fires might portray the optimum packing ratio more accurately than data from moving fire fronts. The results of the current work were merged with Wilson's (1982) data for 0.635- and 1.37-cm (1/4- and 1/2-inch)-thick ponderosa pine sticks to investigate relationship of the fuel bed descriptor $1/\sigma\beta\delta$ and flame length in both stationary and moving fires. Similarly to stationary fires, moving fire fronts do exhibit a drop in flame length as $1/\sigma\beta\delta$ increases beyond 0.22 but maintain low flame height in thin fuels out to approximately 0.80 for $1/\sigma\beta\delta$ (fig. 9). Although similar responses are apparent, loading and moisture content must be studied before the behavior of moving and stationary fires can be fully compared. In addition, burning of fine fuels in a fuel bed of mixed sizes will result in higher flame heights than observed when only fine fuels make up the fuel bed. Because the burnout of the large

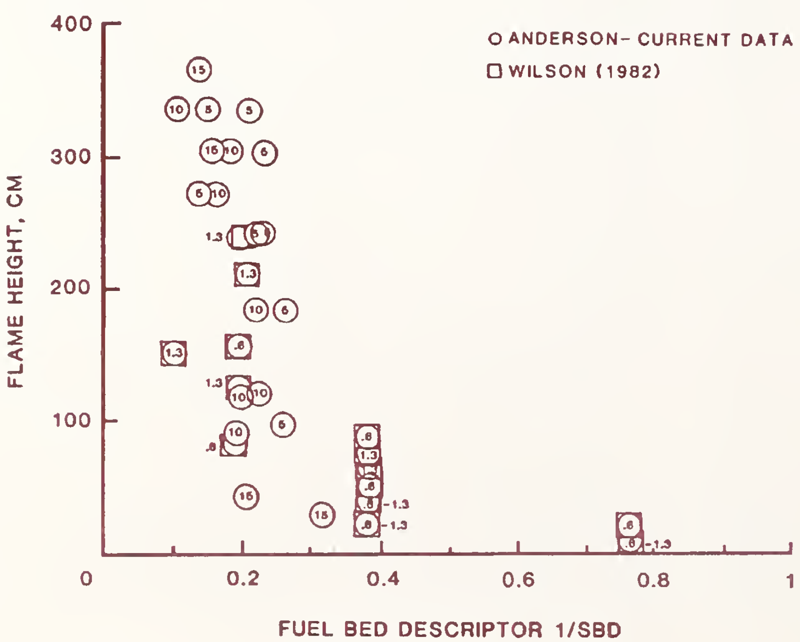

Figure 9—Merging of data from Wilson (1982) with current study data. Plotting shows a sharp decrease in flame length at fuel bed descriptor values at 0.22 and above for both moving and stationary fires. Numbers within the data symbols denote the fuel particle thickness in centimeters.

fuels takes place after the fire front has passed, linking behavior of moving fires and stationary fires could be valuable in assessing the thermal impacts of a wildland fire.

REFERENCES

Albini, F. A. 1976a. Estimating wildfire behavior and effects. Gen. Tech. Rep. INT-30. Ogden, UT: U.S. Department of Agriculture, Forest Service, Intermountain Forest and Range Experiment Station. 91 p.

Albini, F. A. 1976b. Computer-based models of wildland fire behavior: a user's manual. Ogden, UT: U.S. Department of Agriculture, Forest Service, Intermountain Forest and Range Experiment Station. 68 p.

Block, J. A. 1971. Theoretical and experimental study of nonpropagating free-burning fires. In: Proceedings, thirteenth symposium (international) on combustion; 1970 August 23-29; Salt Lake City, UT. Pittsburgh, PA: The Combustion Institute: 971-978.

Delichatsios, M. A. 1976. Fire growth rates in wood cribs. Combustion and Flame. 27: 267-278.

Frandsen, W. H.; Schuette, R. D. 1978. Fuel burning rates of downward vs. horizontally spreading fires. Res. Pap. INT-214. Ogden, UT: U.S. Department of Agriculture, Forest Service, Intermountain Forest and Range Experiment Station. 12 p.

Gross, D. 1962. Experiments on the burning of cross piles of wood. Gaithersburg, MD: National Bureau of Standards.

Harmathy, T. Z. 1972a. A new look at compartment fires, part I. Fire Technology. 8(3): 196-217.

Harmathy, T. Z. 1972b. A new look at compartment fires, part II. Fire Technology. 8(4): 326-354.

Harmathy, T. Z. 1976. Design of buildings for fire safety, part I. Fire Technology. 12(2): 95-103.

Heskestad, G. 1973. Modeling of enclosure fires. In: Proceedings, fourteenth symposium (international) on combustion; 1972 August 20-25; University Park, PA. Pittsburgh, PA: The Combustion Institute: 1021-1030.

Ottmar, R. D. 1987. Prescribed fire and fuel consumption in uncured slash—preliminary results. In: Proceedings, ninth conference on fire and forest meteorology; 1987 April 21-24; San Diego, CA. Boston, MA: American Meteorological Society: 132-136.

Rothermel, R. C. 1972. A mathematical model for predicting fire spread in wildland fuels. Res. Pap. INT-115. Ogden, UT: U.S. Department of Agriculture, Forest Service, Intermountain Forest and Range Experiment Station. 40 p.

Smith, P. C.; Thomas, P. H. 1970. The rate of burning of wood cribs. Fire Technology. 6(1): 29-38.

Thomas, P. H. 1974. Effects of fuel geometry in fires. Boorham Woods, United Kingdom, Current Paper No. 29.

Wilson, R. A., Jr. 1982. A reexamination of fire spread in free-burning porous fuel beds. Res. Pap. INT-289. Ogden, UT: U.S. Department of Agriculture, Forest Service, Intermountain Forest and Range Experiment Station. 28 p.

Anderson, Hal E. 1990. Relationship of fuel size and spacing to combustion characteristics of laboratory fuel cribs. Res. Pap. INT-424. Ogden, UT: U.S. Department of Agriculture, Forest Service, Intermountain Research Station. 9 p.

Flaming combustion in cribs of large woody fuels, thickness 5 cm or greater, is not sustained when fuel spacing ratio, fuel edge-to-edge separation distance to fuel thickness, is greater than 3:1. The flame length associated with the large-fuel burning rate was found to drop rapidly when the large-fuel spacing ratio increases beyond 2.23:1. This supports the critical spacing assigned in the large-fuel subroutine burnout of Albini's fire modeling program.

KEYWORDS: fuels, fire behavior, spacing, burning rates